CrossMark

CASE REPORT

Giant Cell Tumor with Secondary Aneurysmal Bone Cyst Shows Heterogeneous Metabolic Pattern on ^{18}F-FDG PET/CT: A Case Report

Hee Jeong Park[1] · Seong Young Kwon[1] · Sang-Geon Cho[2] · Jahae Kim[2] ·
Ho-Chun Song[2] · Sung Sun Kim[3] · Yeon Hong Yoon[4] · Jin Gyoon Park[5]

Abstract Giant cell tumor (GCT) is a generally benign bone tumor accounting for approximately 5 % of all primary bone neoplasms. Cystic components in GCTs that indicate secondary aneurysmal bone cysts (ABCs) are reported in 14 % of GCTs. Although both of them have been described separately in previous reports that may show considerable fluorodeoxyglucose (FDG) uptake despite their benign nature, the findings of GCT with secondary ABC on ^{18}F-FDG positron emission tomography/ computed tomography (PET/CT) have not been well-known. We report a case of GCT with secondary ABC in a 26-year-old woman. ^{18}F-FDG PET/CT revealed a heterogeneous hypermetabolic lesion in the left proximal femur with the maximum standardized uptake value of 4.7. The solid components of the tumor showed higher FDG uptake than the cystic components. These observations suggest that the ABC components in GCTs show heterogeneous metabolic patterns on ^{18}F-FDG PET/CT.

Introduction

Giant cell tumor (GCT) usually is a benign bone tumor, comprising approximately 18–23 % of benign bone neoplasm [1]. The benign tumors tend to occur in the meta-epiphyseal region of the long bones with extension to subchondral bones [1, 2]. The stroma of most GCTs contain numerous thin-walled vascular channels, often with areas of hemorrhage, and are presumed to be associated with secondary aneurysmal bone cyst (ABC) formation [1, 3]. Cystic components that indicate secondary ABCs are reported in 14 % of GCTs [1].

Here we report the imaging findings for a patient with GCT with ABC determined by radiographs, magnetic resonance imaging (MRI), ^{99m}Tc bone scintigraphy, and [F-18]-fluorodeoxyglucose (^{18}F-FDG) positron emission tomography/computed tomography (PET/CT). To the best of our knowledge, there has been no report of a ^{18}F-FDG PET/ CT finding of GCT with ABC.

Case Report

A 26-year-old woman presented with persistent left-hip pain for 4 months. There was no history of prior trauma to that hip. On physical examination, there was moderate tenderness in the swollen left hip. Radiograph of the hip showed a heterogeneously lucent, expansile bone tumor in the left proximal femur (Fig. 1). Subsequent MRI revealed a 4.2 × 3.6 × 10.1-cm mass with low signal intensity on T1-weighted images and multi-chambered high signal intensity on T2-weighted images (Fig. 2). Giant cell tumor or cavernous hemangioma was
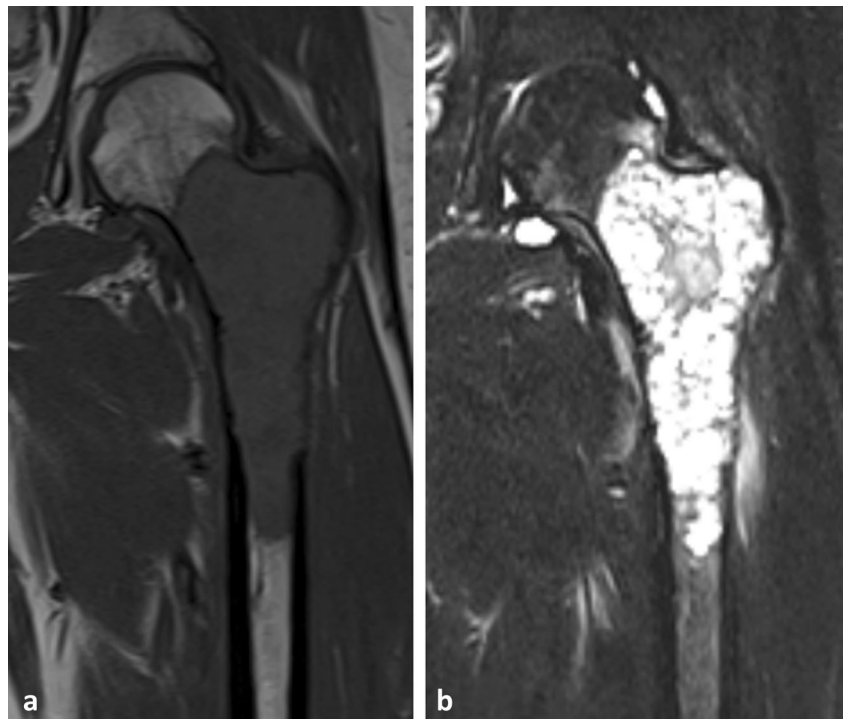
✉ Ho-Chun Song
songhc@jnu.ac.kr

1   Department of Nuclear Medicine, Chonnam National University Hwasun Hospital, Huasun-Gun, Republic of Korea

2   Department of Nuclear Medicine, Chonnam National University Hospital, Gwangju, Republic of Korea

3   Department of Pathology, Chonnam National University Hospital, Gwangju, Republic of Korea

4   Department of Radiology, Chonnam National University Hwasun Hospital, Huasun-Gun, Republic of Korea

5   Department of Radiology, Chonnam National University Hospital, Gwangju, Republic of Korea

Fig. 1 Antero-posterior radiograph of left hip obtained at initial presentation. An expansile, osteolytic lesion is present in the intertrochanteric portion of the left femur. The margin of the lesion is unclear

suggested from the radiographic findings. ^{99m}Tc HDP bone scintigraphy and ^{18}F-FDG PET/CT were performed to exclude malignant bone tumors such as chondrosarcoma. Bone scintigraphy showed unevenly increased uptake, especially in the medial margins of the mass (Fig. 3a). ^{18}F-FDG PET/CT revealed a hypermetabolic lesion in the left proximal femur with the maximum standardized uptake value (SUVmax) of 4.7; SUVmax of the peripheral portion of the tumor was 2.6.

There was no other hypermetabolic lesion considering either primary malignancy or metastasis (Fig. 3b). The patient underwent an open bone biopsy to confirm the diagnosis. Histopathologic examination presented the characteristic findings of a GCT with secondary ABC. Microscopically, the solid components showed evenly distributed multinucleated osteoclast-like giant cells and intervening proliferating mononuclear cells, consistent with GCT (Fig. 4a). Large blood-filled cystic cavities were lined with a cell-rich membrane composed of mononuclear cells and scattered giant cells (Fig. 4b). Surgery was performed for tumor removal, as well as to correct the pathologic fracture. Curettage and reconstruction with tumor prosthesis was performed. The microscopic evaluation of the removed mass was consistent with GCT with secondary ABC.

Discussion

GCT is a common primary bone tumor that occurs predominantly in the meta-epiphyseal regions of long bones, typically in the distal femur and the proximal tibia (50–65 %) [2]. GCTs in bone usually occur after skeletal maturity; peak incidence is between 20–40 years of age. The sex distribution shows a slight predominance in females (1.3:1 = female:male) [1]. Histopathologically, GCT shows uniformly scattered multinucleated giant cells that resemble osteoclasts in a background of mononuclear cells. Giant and mononuclear cells show similar nuclear features; they are both round, oval, or polygonal in shape and may resemble normal histiocytes [4].

Fig. 2 Coronal T1-weighted MR image (**a**) shows a low-signal-intensity lesion in the left femur. Coronal fat-suppressed T2-weighted MR image (**b**) shows multichambered high signal intensity

Fig. 3 ^{99m}Tc HDP whole-body bone scintigraphy (**a**) demonstrates unevenly increased uptake, especially in the peripheral margin of the mass of the left proximal femur. Coronal MIP and fusion ¹⁸F-FDG PET/CT image (**b**) show abnormal uptake in the left proximal femur. SUVmax of the lesion is 4.7. No evidence of other hypermetabolic lesion is observed
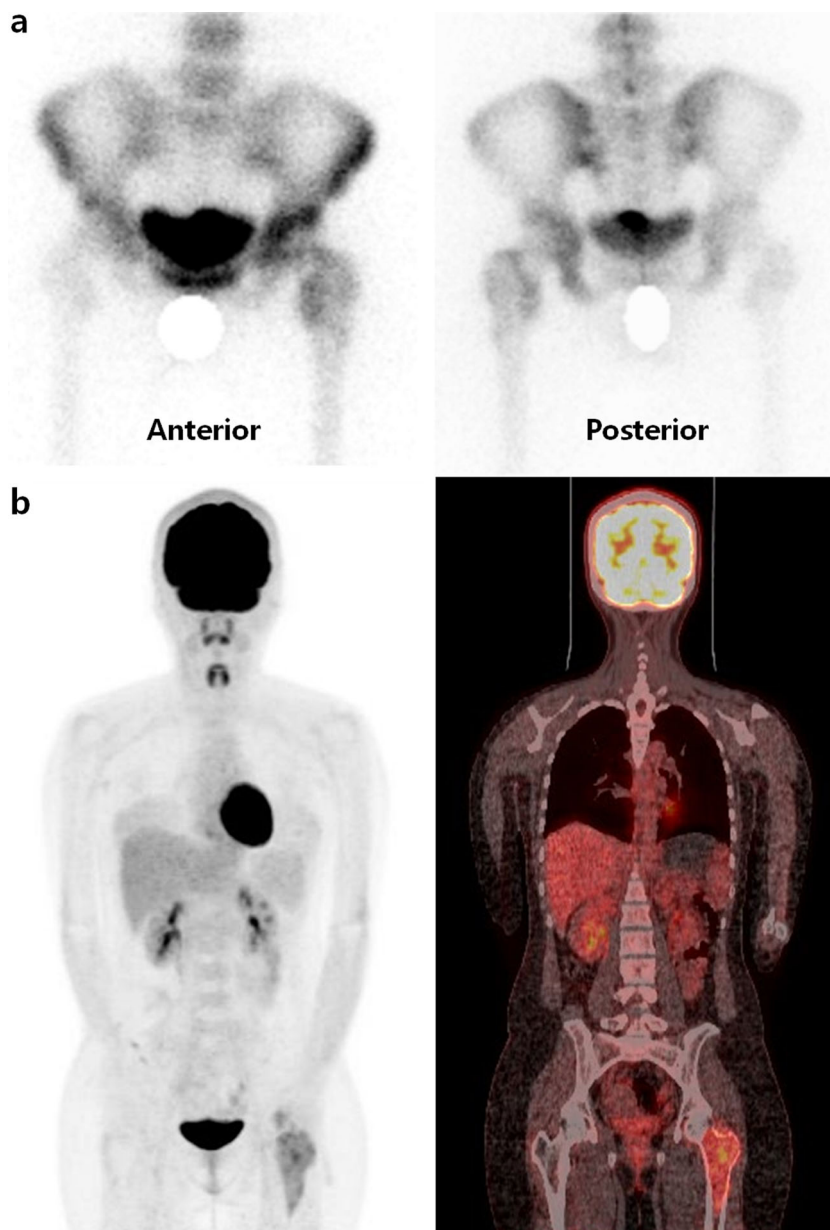
Radiographically, GCTs typically present as eccentrically located, lucent lesions that lack matrix mineralization. Cortical thinning, cortical penetration (33–50 %), periosteal reaction (10–30 %), and pathologic fracture (11–37 %) may be present [1, 5]. In bone scintigraphy, most GCTs and ABCs reveal increased uptake, especially around the periphery, with a central photopenic region (doughnut sign). Blood pool imaging also shows increased uptake, although usually to a lesser degree than in delayed imaging. Increased radiotracer uptake in adjacent bones and joints is common (62 % of cases) because of increased blood flow and disuse osteoporosis [6, 7]. In this case, bone scintigraphy showed increased uptake in the medial margins compared with the central portion of the tumor. This was an atypical imaging feature for either GCT or ABC, and

the mixture of ABC components in the GCT may have contributed to this nonspecific feature.

An ABC is a benign expansile, non-neoplastic, tumor-like lesion with a distinct bony shell and osseous septation. Lichtenstein [8] described ABCs as reactive lesions rather than true neoplasms and stated that vascular disturbances in bone lead to increased intraosseous pressure, causing destruction and expansion of bone. Primary ABCs account for 1.4 % of all primary bone tumors. Thirty to fifty percent of ABCs occur secondary to primary tumors, such as GCT, chondroblastoma, chondromyxoid fibroma, fibrous dysplasia, and osteosarcoma; GCT is the most common [9]. Histologically, ABCs have a biphasic pattern with cystic (95 %) and solid (5 %) areas. The cystic areas typically show
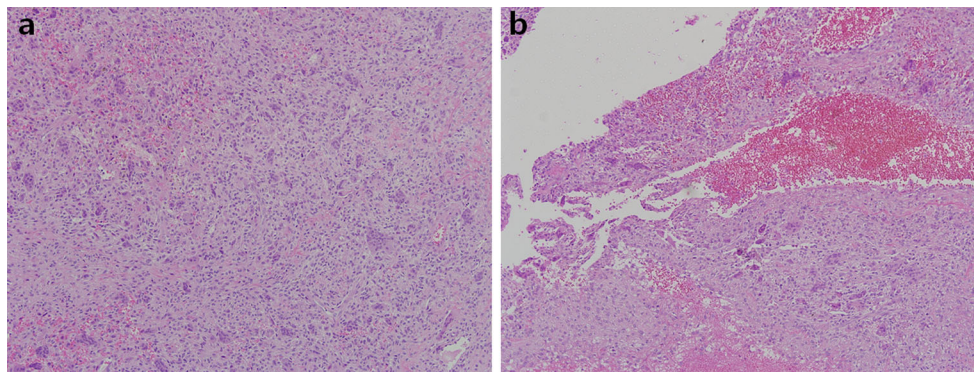
Fig. 4 Microscopic findings of the resected tumor. **a** Solid components of GCT reveal a sheet of mononuclear stromal cells and evenly scattered osteoclast-like multinucleated giant cells. **b** Cystic aneurysmal components show blood-filled cystic cavities lined with a thick membranous structure that comprises multinucleated giant cells and mononuclear cells (H & E stain; original magnification: **a** ×100, **b** ×100)

cavernomatous spaces filled with unclotted blood among bony trabeculae and are separated by fibrous septa composed of abundant fibroblasts, spindle-shaped stromal cells, osteoclast-type giant cells, and reactive woven bone. The solid areas consist of spindle-shaped stromal cells, proliferating blood vessels, mononuclear cells, and some interspersed multinucleated giant cells [10, 11]. ABCs and GCTs share some histologic features, such as multinucleated giant cells and stromal cells; however, ABCs often reveal clusters of giant cells (not evenly distributed), strands of bone, stromal hemorrhage, and calcifying matrix.

ABC components frequently reveal fluid-fluid levels. They may show variable signal intensity on T1-weighted MR imaging and markedly increased signal intensity on T2-weighted MRI [1, 12]. The solid components of GCTs show low to intermediate signal intensity on T1-weighted images and heterogeneous high signals in areas of low signal intensity (variable) on T2-weighted images because of either hemosiderin or fibrosis [1, 13]. The solid regions of GCTs show diffuse enhancement after intravenous gadolinium infusion, reflecting the hypervascular tissue seen on pathologic analysis, and this finding helps to differentiate GCT regions from ABC regions [1].

A review of the literature suggests that giant cell-containing lesions such as GCTs and ABCs may show high uptake on ^{18}F-FDG PET/CT study [14, 15]. The average
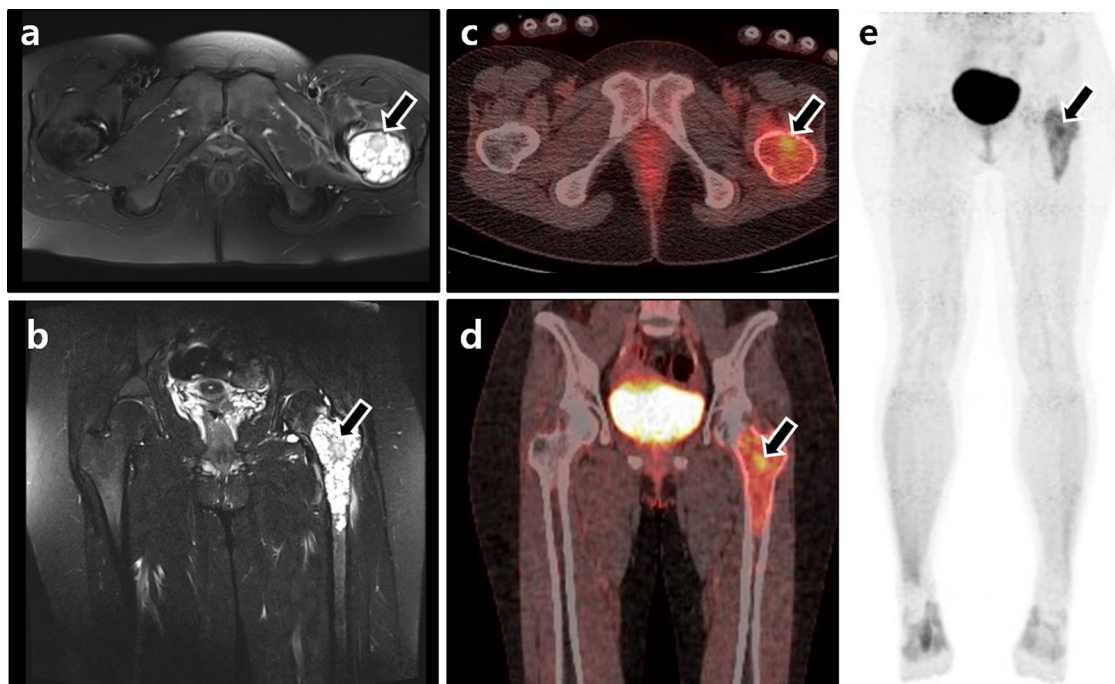

Fig. 5 Correlation of the lesion with MRI and ^{18}F-FDG PET/CT. Fat-suppressed T2-weighted MR images (**a**, **b**) show less high signal intensity on solid portion (*arrow*) than cystic portion of the lesion. Fusion (**c**, **d**) and maximal intensity projection image (**e**) of ^{18}F-FDG PET/CT reveal higher uptake on solid portion than cystic portion

SUVmax of GCTs has been reported to be 8.8 [16] (range 4.6–11.2) [14–17]. Folpe et al. [17] suggested that elevated SUV is correlated with high cellularity and proliferative activity in GCTs. Hoshi et al. [16] found that hexokinase-2, a key enzyme in the glycolytic pathway in tumor cells, was strongly expressed in the cytoplasm of giant and spindle GCT cells and contributed significantly to FDG accumulation. Although ABCs also contain giant cells and fibroblasts, which are known to show a relatively high accumulation of FDG [18], the reported SUVmax on ^{18}F-FDG PET/CT has been found to be lower than that for GCTs (average, 3.0; range, 1.1–5.9) [19, 20]. We suggest that the low cellularity of ABCs may be one contributor to decreased SUV [21]. In this case, FDG uptake in the solid portion of the lesion (SUVmax = 4.7) was higher than that in the cystic portion (SUVmax = 2.6) (Fig. 5), and the distribution of ABC components in the GCT appeared to be the cause of this heterogeneous metabolic pattern.

We believe that this report is the first to describe the appearance of a GCT with ABC on ^{18}F-FDG PET/CT. GCTs with ABCs may show heterogeneous metabolic patterns with relatively low FDG uptake compared with average GCT values on ^{18}F-FDG PET/CT.

Compliance with Ethical Standards

References

1. Murphey MD, Nomikos GC, Flemming DJ, Gannon FH, Temple HT, Kransdorf MJ. Imaging of giant cell tumor and giant cell reparative granuloma of bone: radiologic-pathologic correlation. Radiographics. 2001;21:1283–309.

2. Campanacci M, Baldini N, Boriani S, Sudanese A. Giant-cell tumor of bone. J Bone Joint Surg Am. 1987;69:106–14.

3. Vincent J, Vigorita V. Bone cysts and giant-cell tumor. Orthopedic Pathology. 2nd ed. Philadelphia: Lippincott Williams & Wilkins; 2007.

4. Werner M. Giant cell tumour of bone: morphological, biological and histogenetical aspects. Int Orthop. 2006;30:484–9.

5. Sherwani RK, Zaheer S, Sabir AB, Goel S. Giant cell tumor along with secondary aneurysmal bone cyst of scapula: a rare presentation. Int J Shoulder Surg. 2008;2:59–61.

6. Levine E, De Smet AA, Neff JR. Role of radiologic imaging in management planning of giant cell tumor of bone. Skeletal Radiol. 1984;12:79–89.

7. Van Nostrand D, Madewell JE, McNiesh LM, Kyle RW, Sweet D. Radionuclide bone scanning in giant cell tumor. J Nucl Med. 1986;27:329–38.

8. Lichtenstein L. Aneurysmal bone cyst. A pathological entity commonly mistaken for giant-cell tumor and occasionally for hemangioma and osteogenic sarcoma. Cancer. 1950;3:279–89.

9. Unni KK, Inwards CY. Dahlin's bone tumors: general aspects and data on 10,165 cases. Philadelphia: Lippincott Williams & Wilkins; 2010.

10. Liu S, Jassim A, Bleeker J, Chen F, Kolanuvada B, Rong R, et al. Histopathological features of aneurysmal bone cyst of the temporal bone—a case report and review of literature. N A J Med Sci. 2015;8:46–9.

11. Rapp TB, Ward JP, Alaia MJ. Aneurysmal bone cyst. J Am Acad Orthop Surg. 2012;20:233–41.

12. Abdelwahab IF, Kenan S, Hermann G, Klein MJ, Lewis MM. Case report 845. Skeletal Radiol. 1994;23:317–9.

13. Pereira HM, Marchiori E, Severo A. Magnetic resonance imaging aspects of giant-cell tumours of bone. J Med Imaging Radiat Oncol. 2014;58:674–8.

14. Aoki J, Watanabe H, Shinozaki T, Takagishi K, Ishijima H, Oya N, et al. FDG PET of primary benign and malignant bone tumors: standardized uptake value in 52 lesions. Radiology. 2001;219: 774–7.

15. Aoki J, Endo K, Watanabe H, Shinozaki T, Yanagawa T, Ahmed AR, et al. FDG-PET for evaluating musculoskeletal tumors: a review. J Orthop Sci. 2003;8:435–41.

16. Hoshi M, Takada J, Oebisu N, Hata K, Ieguchi M, Nakamura H. Overexpression of hexokinase-2 in giant cell tumor of bone is associated with false positive in bone tumor on FDG-PET/CT. Arch Orthop Trauma Surg. 2012;132:1561–8.

17. Folpe AL, Lyles RH, Sprouse JT, Conrad 3rd EU, Eary JF. (F-18) fluorodeoxyglucose positron emission tomography as a predictor of pathologic grade and other prognostic variables in bone and soft tissue sarcoma. Clin Cancer Res. 2000;6:1279–87.

18. Kubota K, Kubota R, Yamada S. FDG accumulation in tumor tissue. J Nucl Med. 1993;34:419–21.

19. Schulte M, Brecht-Krauss D, Heymer B, Guhlmann A, Hartwig E, Sarkar MR, et al. Grading of tumors and tumorlike lesions of bone: evaluation by FDG PET. J Nucl Med. 2000;41:1695–701.

20. Kole AC, Nieweg OE, Hoekstra HJ, van Horn JR. Fluorine-18-fluorodeoxyglucose assessment of glucose metabolism in bone tumors. J Nucl Med. 1998;39:810–5.

21. Higashi K, Clavo AC, Wahl RL. Does FDG uptake measure proliferative activity of human cancer cells? In vitro comparison with DNA flow cytometry and tritiated thymidine uptake. J Nucl Med. 1993;34:414–9.